Electronic Supplementary Material (ESI) for Physical Chemistry Chemical Physics.

Supporting Information

Anchoring of a hydrophobic heptapeptide (AFILPTG) on silica facilitates peptide unfolding at the abiotic-biotic

Victor V. Volkov,[a] Hendrik Heinz[b] and Carole C. Perry[a]*

[a] Interdisciplinary Biomedical Research Centre, School of Science and Technology, Nottingham Trent University, Clifton Lane, Nottingham NG11 8NS, United Kingdom.
[b] Chemical and Biological Engineering, College of Engineering & Applied Science,
University of Colorado Boulder, Boulder, Colorado 80309, USA

To extract representative structural cases for the polypeptide when next to silica, we select N-terminal (the mean coordinate for N atom and three Hydrogen atoms connected to it); centre of the phenylalanine side group, threonine side groups; and the C-terminal (the mean coordinates for C atom and two Oxygen atoms connected to it (red line) to monitor distances between the selected structural moieties silica surface along the MD trajectories: see Figure S1. The anticipated placements of the referenced structural moieties in respect to interface allowed us to narrow to structural cases along the MD trajectories, which may be considered as states when polypeptide is associated with silica.

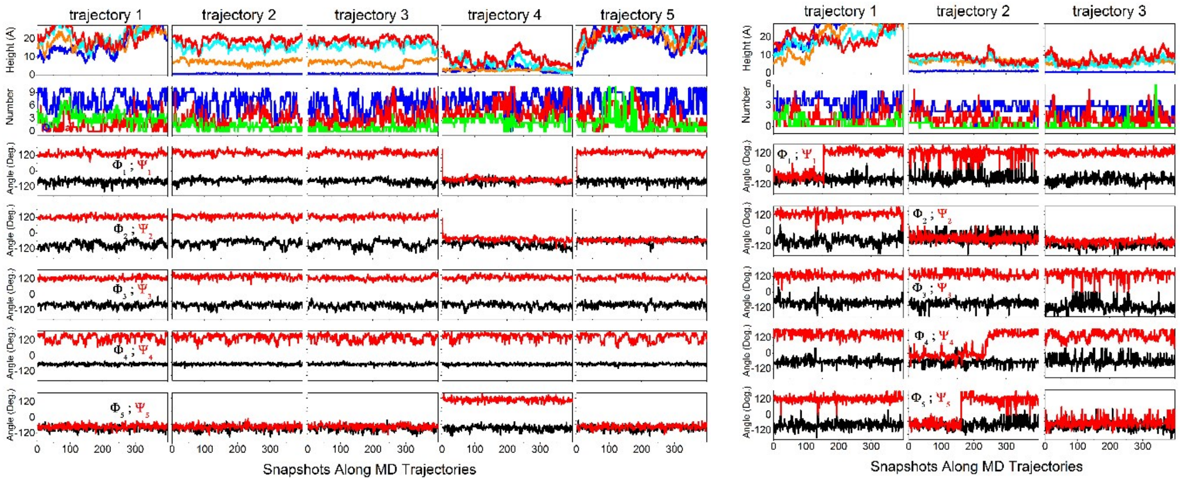

Figure S1. *Structural properties of the polypeptide according to five AF82 trajectories (left set) and three AF91 trajectories (right set) as indicated. Upper Row: Heights of N-terminal, side groups of phenylalanine, threonine, and C-terminal (by Blue, Orange, Cyan and Red lines, respectively) above the mean (along the Z axis of the box) of H atom distribution at SiO_2 interface. Number of Na+ and SiO- within the cut-off radius around the polypeptide (Red and Blue lines, respectively); Green line shows number of Na+ within the cut-off radius around the polypeptide and proximal to the interface. The other Rows: numeric values of {Φ; Ψ} angular pairs counted from N to C terminal (from top to bottom).*

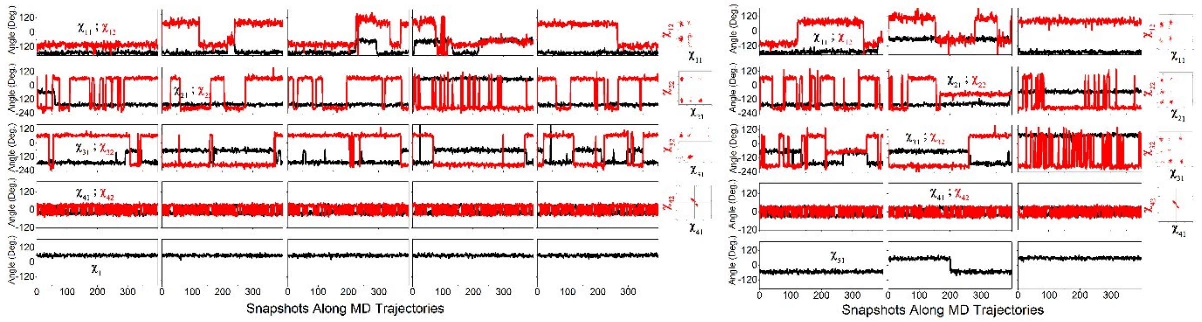

Figure S2. *Dihedral angles* χ_1 (black) and χ_2 (red) *of the side groups of* phenylalanine, isoleucine, leucine, proline and threonine (from left to right) *according to five AF82 trajectories (left-side set) and three AF91 trajectories (right-side set), as indicated.*

Additionally, in Figures S1 and S2 we show the dihedral angles of the polypeptide backbone and the χ_1 and χ_2 dihedral angles of the side groups of phenylalanine, isoleucine, leucine, proline and threonine.

χ_1 angle is determined by N, Cα, C_β and X atoms of a selected aminoacids. Here, X = CG for phenylalanine, leucine and proline; X = CG1 for isoleucine; X = OG for threonine.

χ_2 angle is determined by Cα, C_β, X, Y and atoms of a selected aminoacids. Here, X = CG for phenylalanine, leucine and proline; X = CG1 for isoleucine; Y= CD for isoleucine and proline; Y= CD1 for phenylalanine and leucine.

The extracted dihedral angles for the simulated backbone realizations and for the side group orientations allow to focus on unique simulated structural states: see Figure S3.

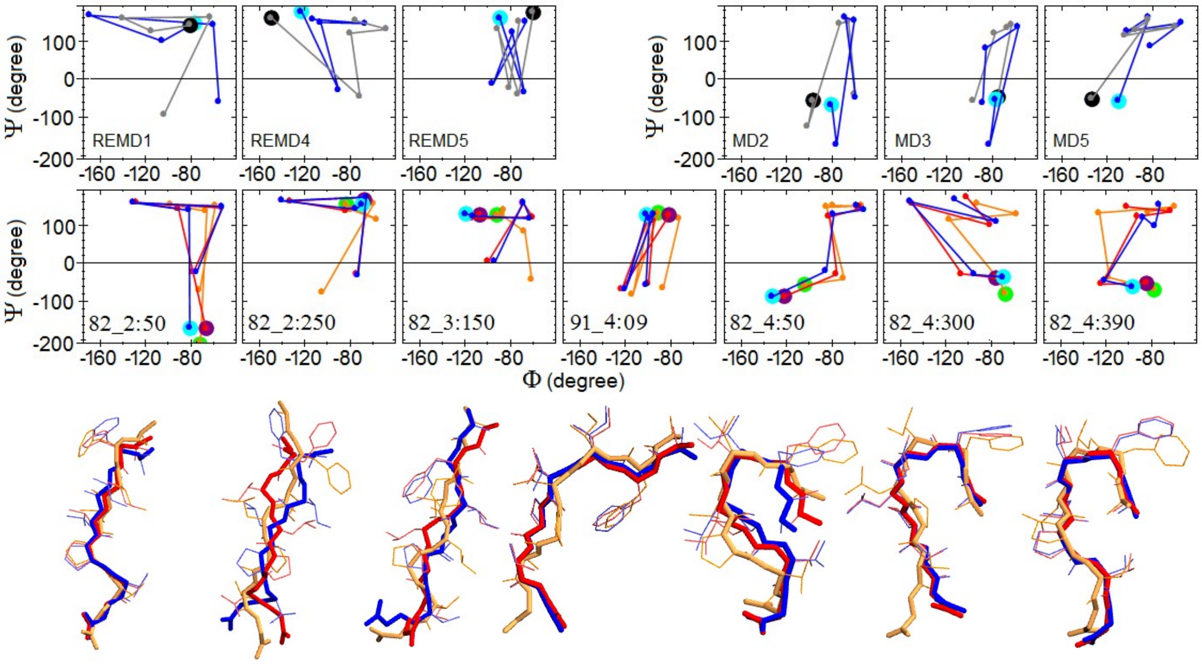

Figure S3. *Structural properties of considered composites as extracted from MD and after optimization with DFT.* ***Upper row:*** *dihedral angles of the five residues (from the N-terminal to the C-terminal) in the expanded region of the Ramachandran angular space for the extracted backbones from the REMD/MD simulations in water (blue line), and after DFT optimizations (grey line); black and cyan* *circles indicate the dihedral angles for the first (from the N terminal) residue.* ***Middle row:*** *dihedral angles of the five residues (from the N-terminal to the C-terminal) in the expanded region of the Ramachandran angular space for the extracted backbones from the MD simulations at silica (light yellow line), after first and second DFT optimizations (red and blue lines, respectively); green, purple and cyan circles indicate the dihedral angles for the first (from the N terminal) residue.* ***Lower row:*** *backbones of the polypeptide in the representative structures upon extractions from MD (light yellow), after first DFT optimization when at* SiO_2 *(red), and after second DFT optimization when alone after removal of the* SiO_2 *(blue).*

To calculate spectral responses, we conduct structural optimizations with DFT implemented in the Gaussian 09 package. A special care was taken to avoid proton transfer events upon pre-optimizations with Hartree-Fock. In the next step we employ the restricted B3LYP functional with 6-31G* basis sets to conduct further optimization, to extract the normal modes, transition dipole moments, Raman tensors and CD transitions.

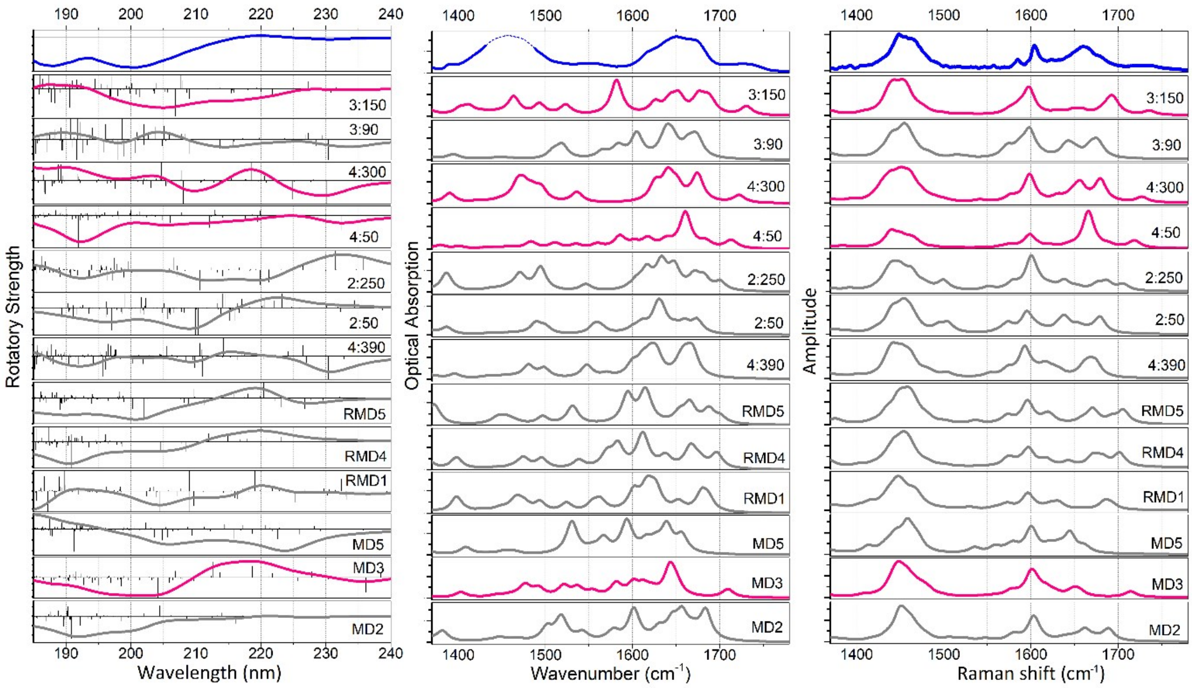

Figure S4. *Blue dispersions at the top are the experimental CD, Raman and FTIR spectra for the AF polypeptide in water. DFT predictions for CD, Raman and IR spectral responses for the computed AF structural cases in water alone: grey colour spectra are discriminated in fitting as inconsistent with experiment; pink colour spectra are considered as possible contributions; cyan colour spectra are marginal, but are still accounted upon fitting.*

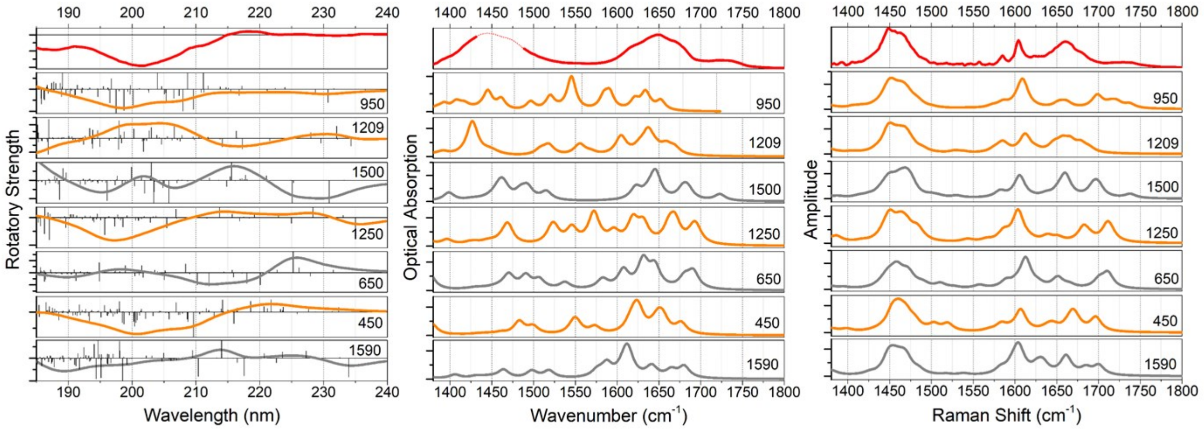

Figure S5. *Red color spectra are the CD, IR and Raman spectra (from left to right) for the AF polypeptide when next to silica. DFT predictions for CD, Raman and IR spectral responses for the AF structural cases computed next to silica: grey colour spectra are discriminated in fitting as inconsistent with the experimental; orange colour spectra are considered as possible contributions.*

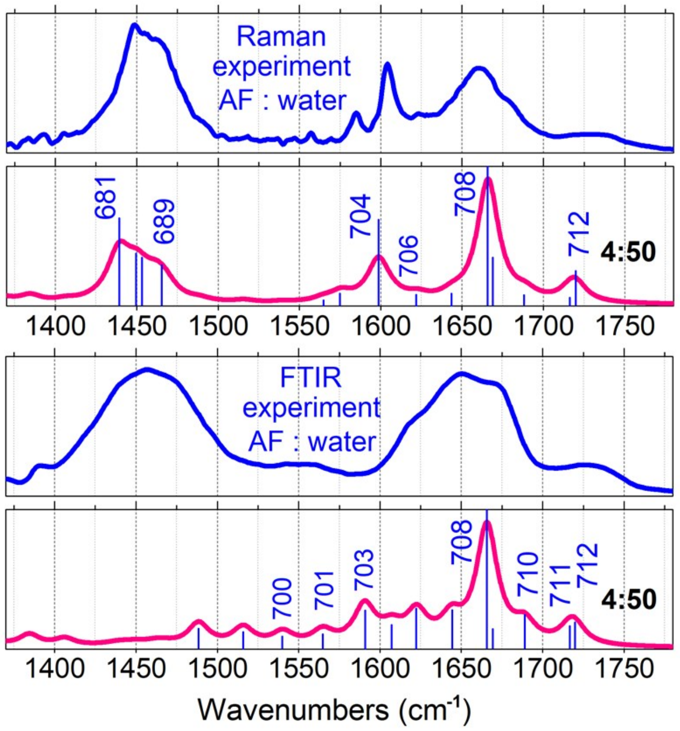

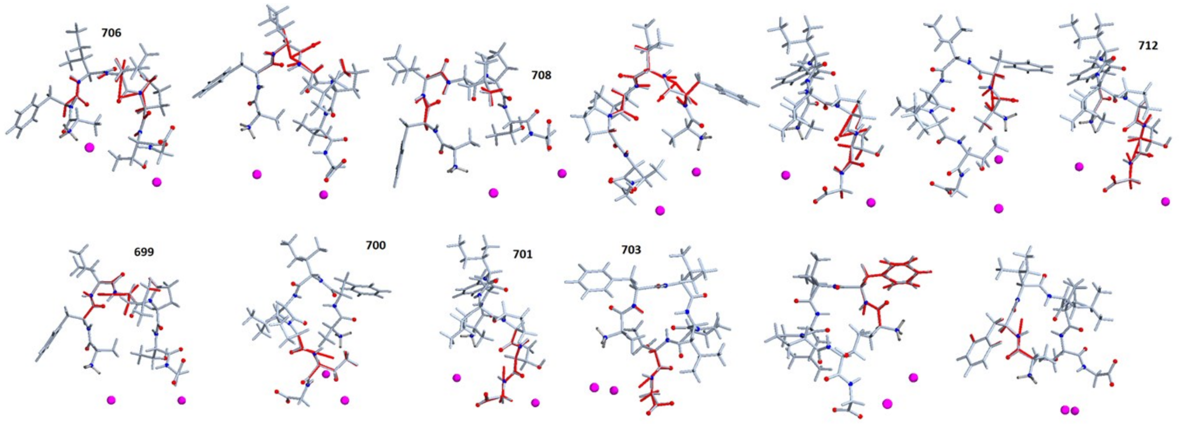

Figure S6. *Experimental Raman and FTIR spectra for the AF polypeptide in water (blue line dispersions); DFT predictions of the responses of the computed aqueous AF structural case AF82_4:50 (purple line dispersions). Vertical blue lines in the panels of the computed dispersions indicate intensities and scaled frequencies of the relevant computed normal modes as described in the visual presentations below according to the normal mode numbering as computed for the structure. Magenta spheres indicate position of Na$^+$. For clarity of normal mode demonstrations, we removed water molecules.*

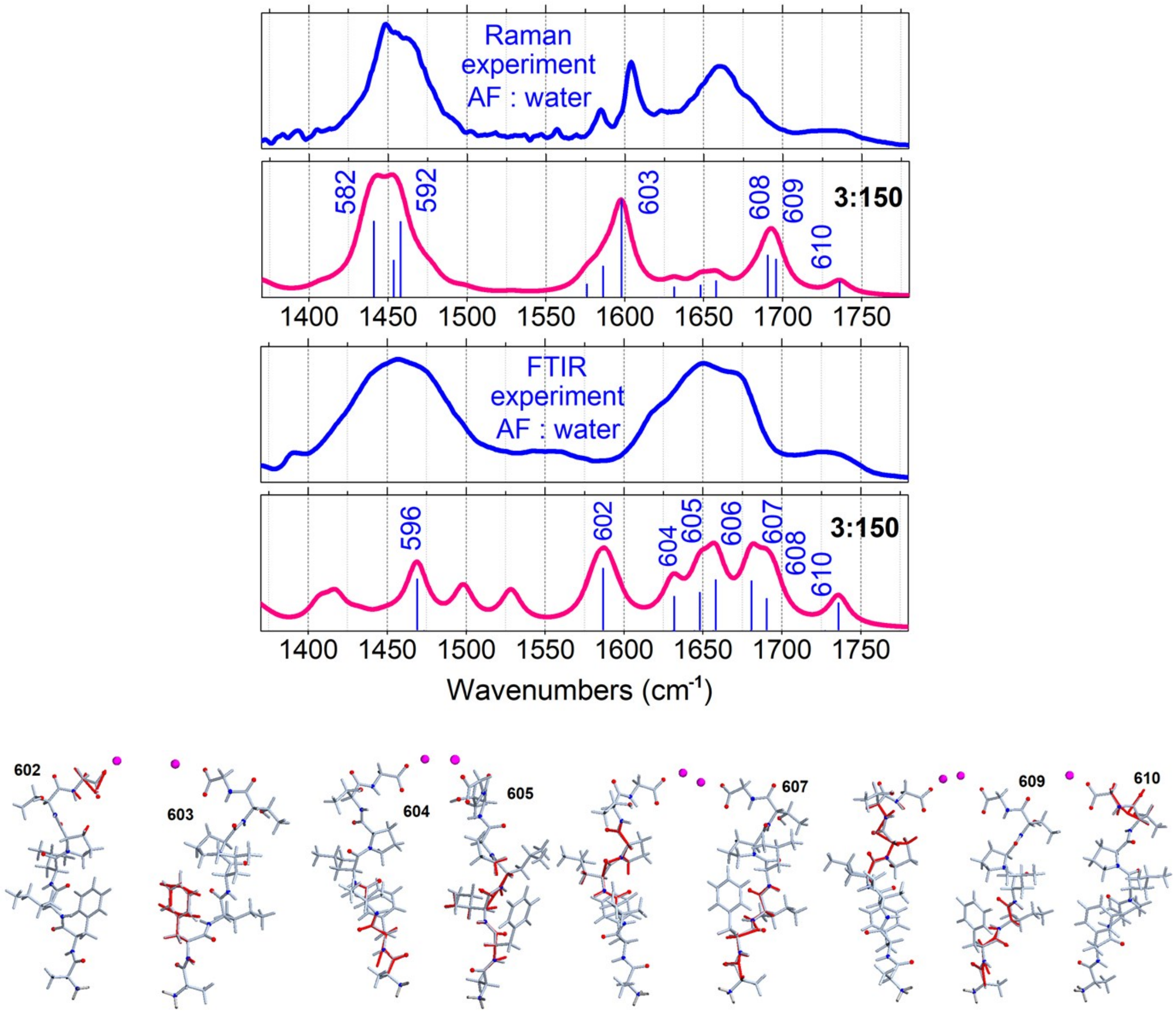

Figure S7. *Experimental Raman and FTIR spectra for the AF polypeptide in water (blue line dispersions); DFT predictions of the responses of the computed aqueous AF structural case AF82_3:150 (purple line dispersions). Vertical blue lines in the panels of the computed dispersions indicate intensities and scaled frequencies of the relevant computed normal modes as described in the visual presentations below according to the normal mode numbering as computed for the structure. Magenta spheres indicate position of Na^{+}. For clarity of normal mode demonstrations, we removed water molecules.*

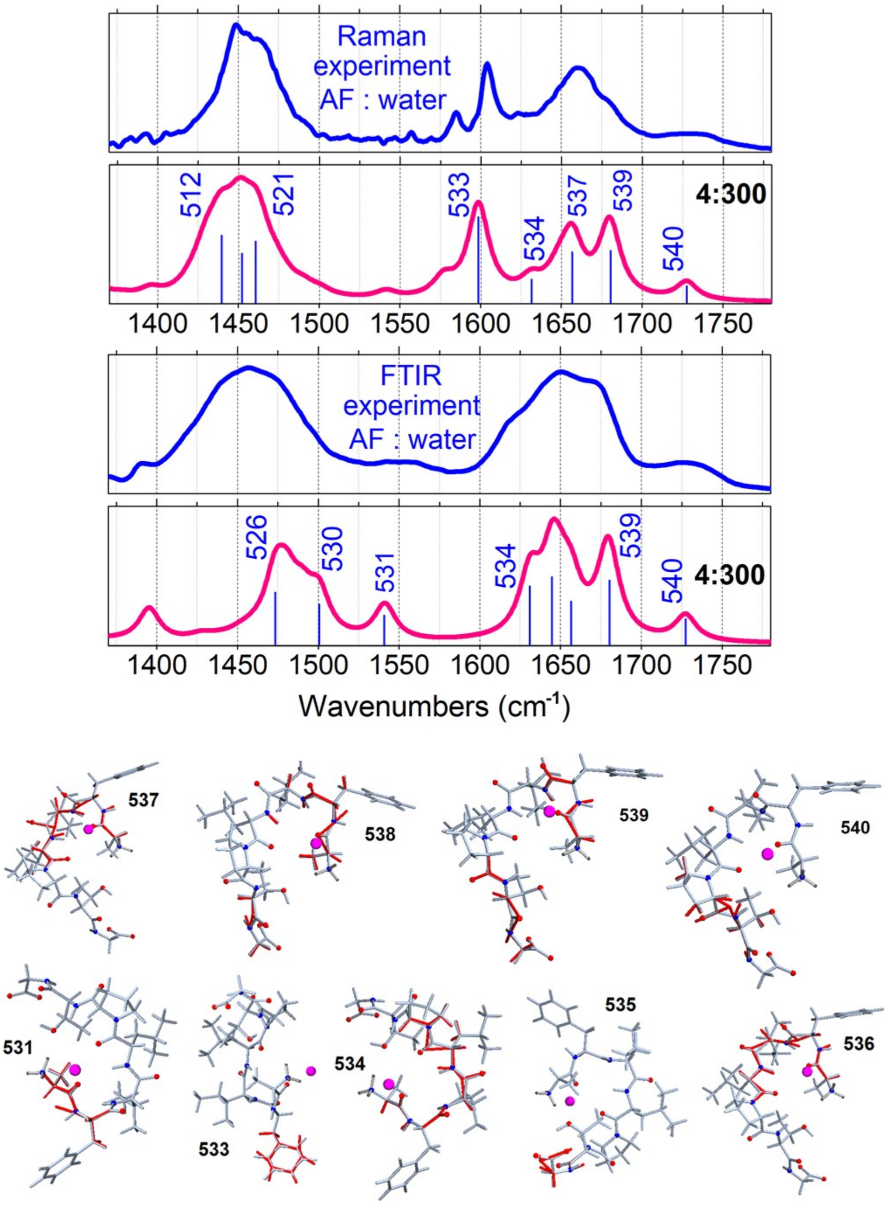

Figure S8. *Experimental Raman and FTIR spectra for the AF polypeptide in water (blue line dispersions); DFT predictions of the responses of the computed aqueous AF structural case AF82_4:300 (purple line dispersions). Vertical blue lines in the panels of the computed dispersions indicate intensities and scaled frequencies of the relevant computed normal modes as described in the visual presentations below according to the normal mode numbering as computed for the structure. Magenta spheres indicate position of* Na^+*. For clarity of normal mode demonstrations, we removed water molecules.*

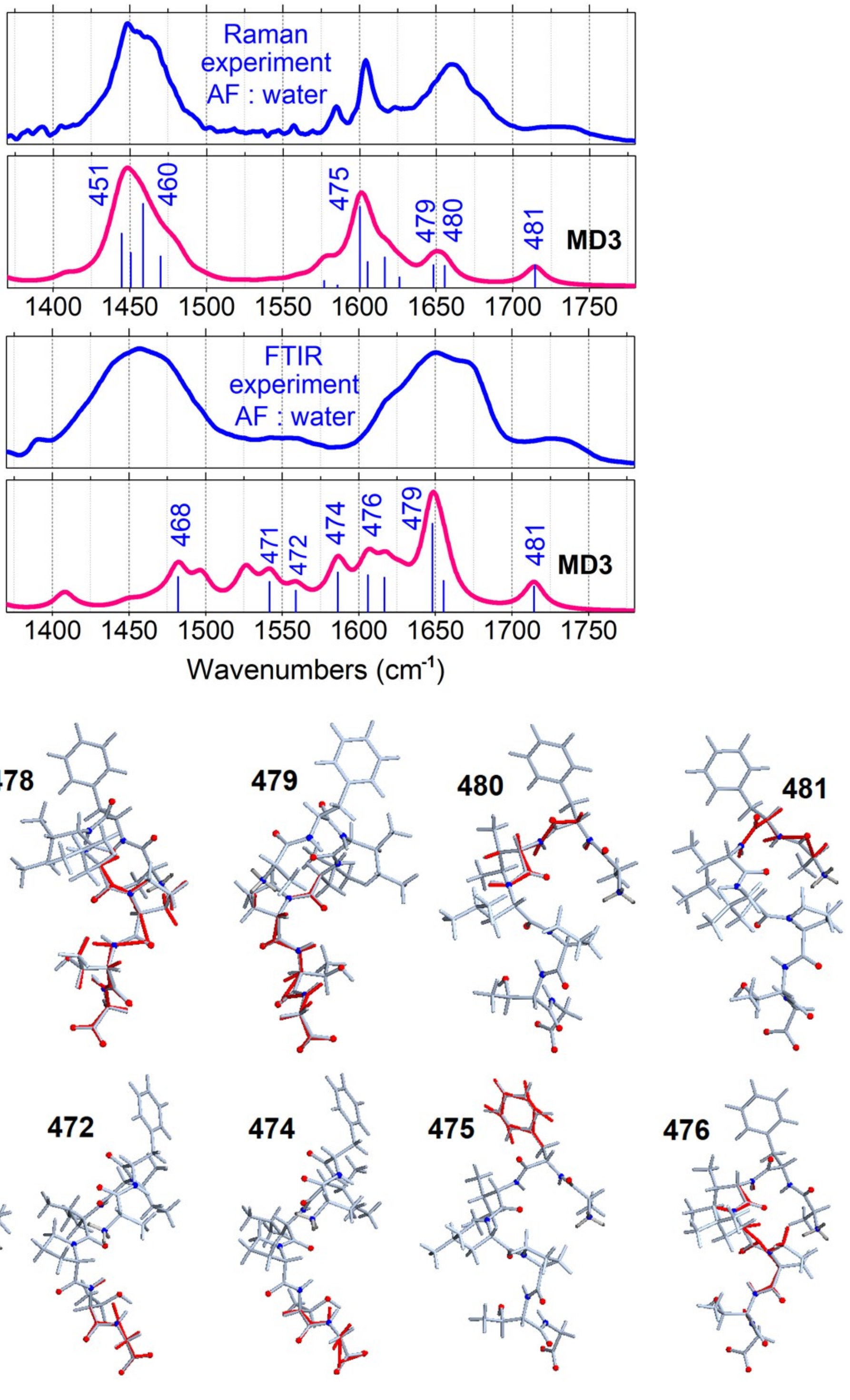

Figure S9. *Experimental Raman and FTIR spectra for the AF polypeptide in water (blue line dispersions); DFT predictions of the responses of the computed aqueous AF structural case MD3 (purple line dispersions). Vertical blue lines in the panels of the computed dispersions indicate intensities and scaled frequencies of the relevant computed normal modes as described in the visual presentations below according to the normal mode numbering as computed for the structure. For clarity of normal mode demonstrations, we removed water molecules.*

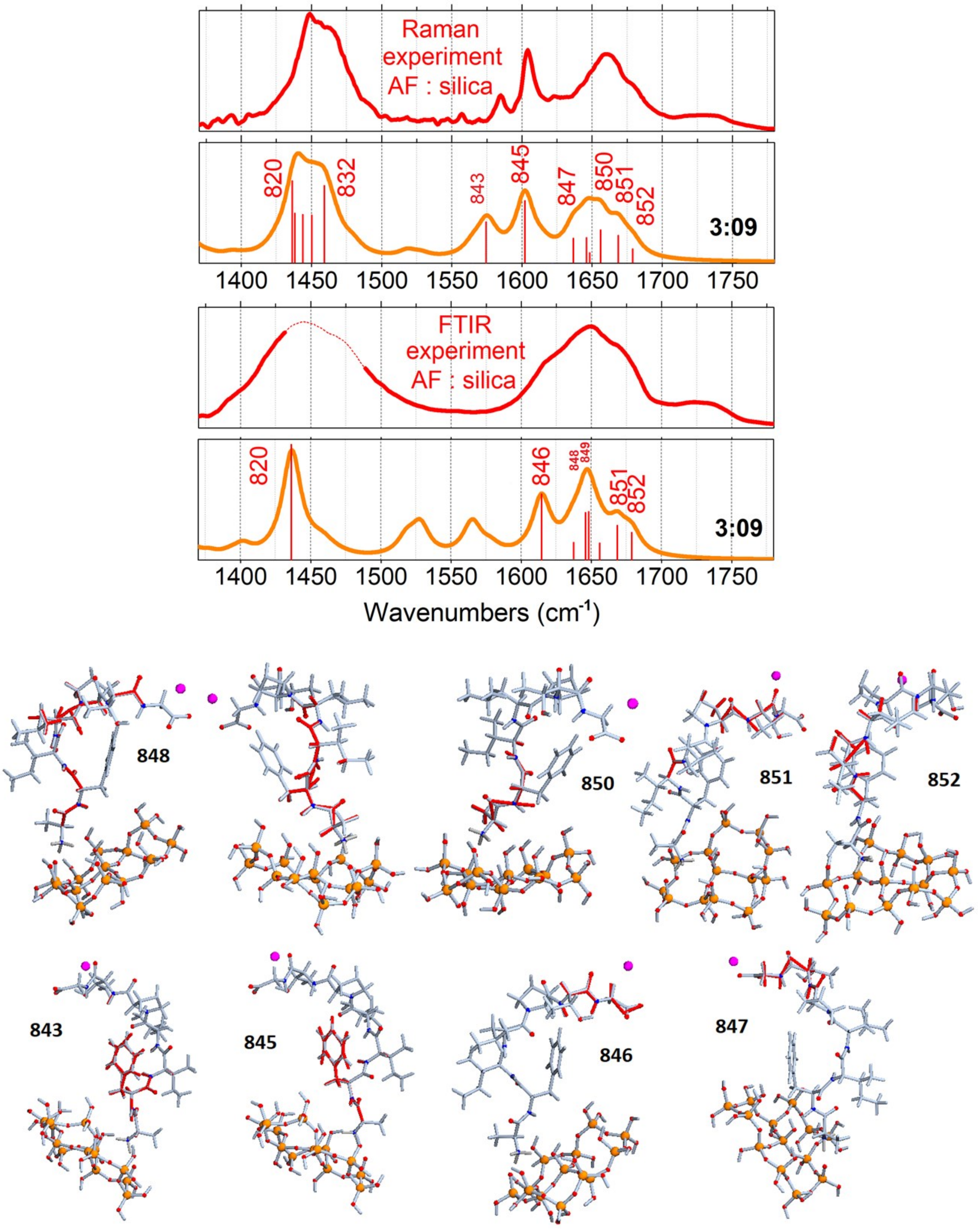

Figure S10. *Experimental Raman and FTIR spectra for the AF polypeptide in presence of silica nanoparticles (red dispersions); DFT predictions of the responses of the computed structural case AF91_3:09 at silica surface (orange line dispersions). Vertical red lines in the panels of the computed dispersions indicate intensities and scaled frequencies of the relevant computed normal modes as described in the visual presentations below according to the normal mode numbering as computed for the structure. Orange and magenta spheres indicate position of silica atoms and Na$^+$, respectively. For clarity of normal mode demonstrations, we removed water molecules.*

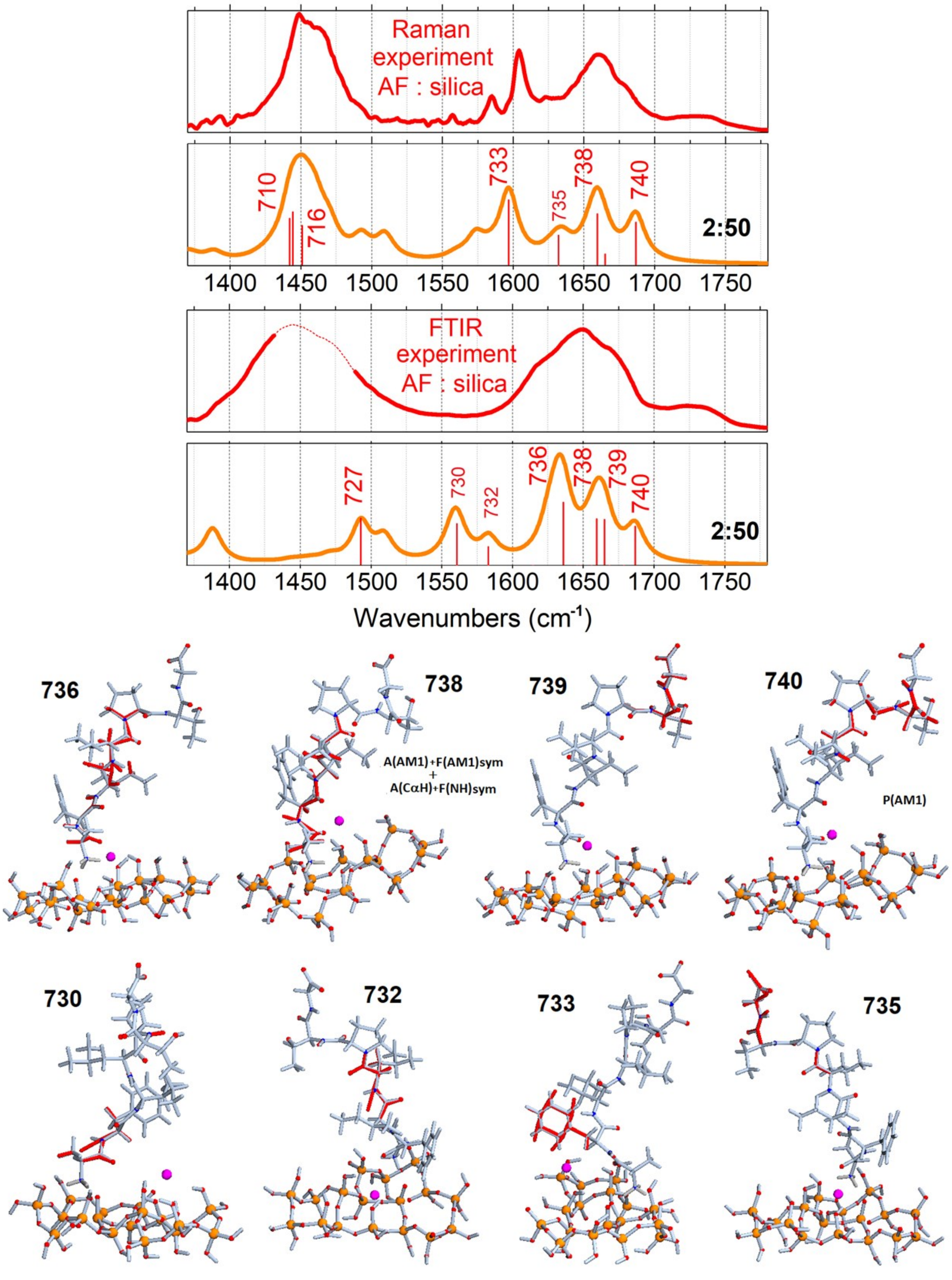

Figure S11. *Experimental Raman and FTIR spectra for the AF polypeptide in presence of silica nanoparticles (red dispersions); DFT predictions of the responses of the computed structural case AF82_2:50 at silica surface (orange line dispersions). Vertical red lines in the panels of the computed dispersions indicate intensities and scaled frequencies of the relevant computed normal modes as described in the visual presentations below according to the normal mode numbering as computed for the structure. Orange and magenta spheres indicate position of silica atoms and Na^{+}, respectively. For clarity of normal mode demonstrations, we removed water molecules.*

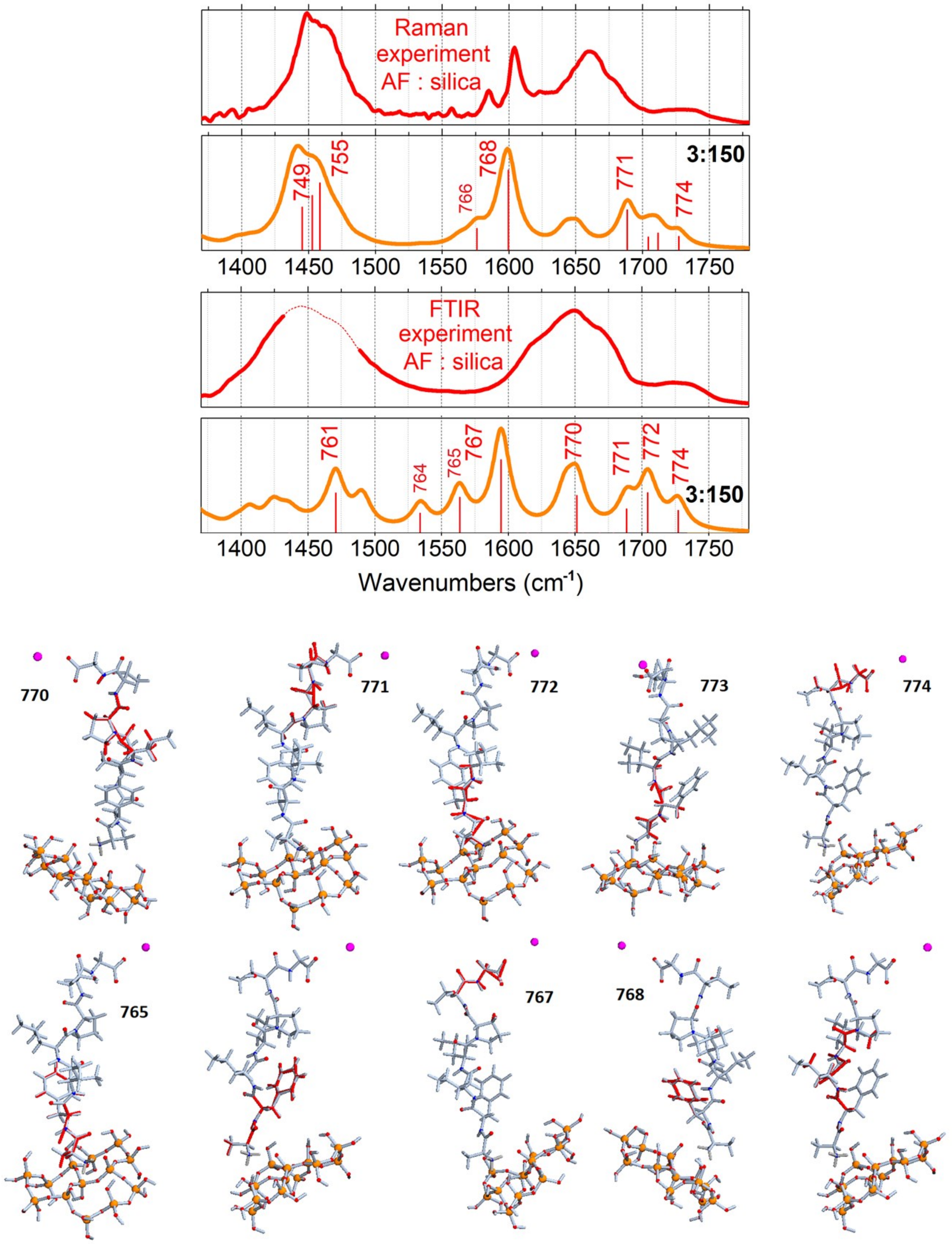

Figure S12. *Experimental Raman and FTIR spectra for the AF polypeptide in presence of silica nanoparticles (red dispersions); DFT predictions of the responses of the computed structural case AF82_3:150 at silica surface (orange line dispersions). Vertical red lines in the panels of the computed dispersions indicate intensities and scaled frequencies of the relevant computed normal modes as described in the visual presentations below according to the normal mode numbering as computed for the structure. Orange and magenta spheres indicate position of silica atoms and* Na^+*, respectively. For clarity of normal mode demonstrations, we removed water molecules.*

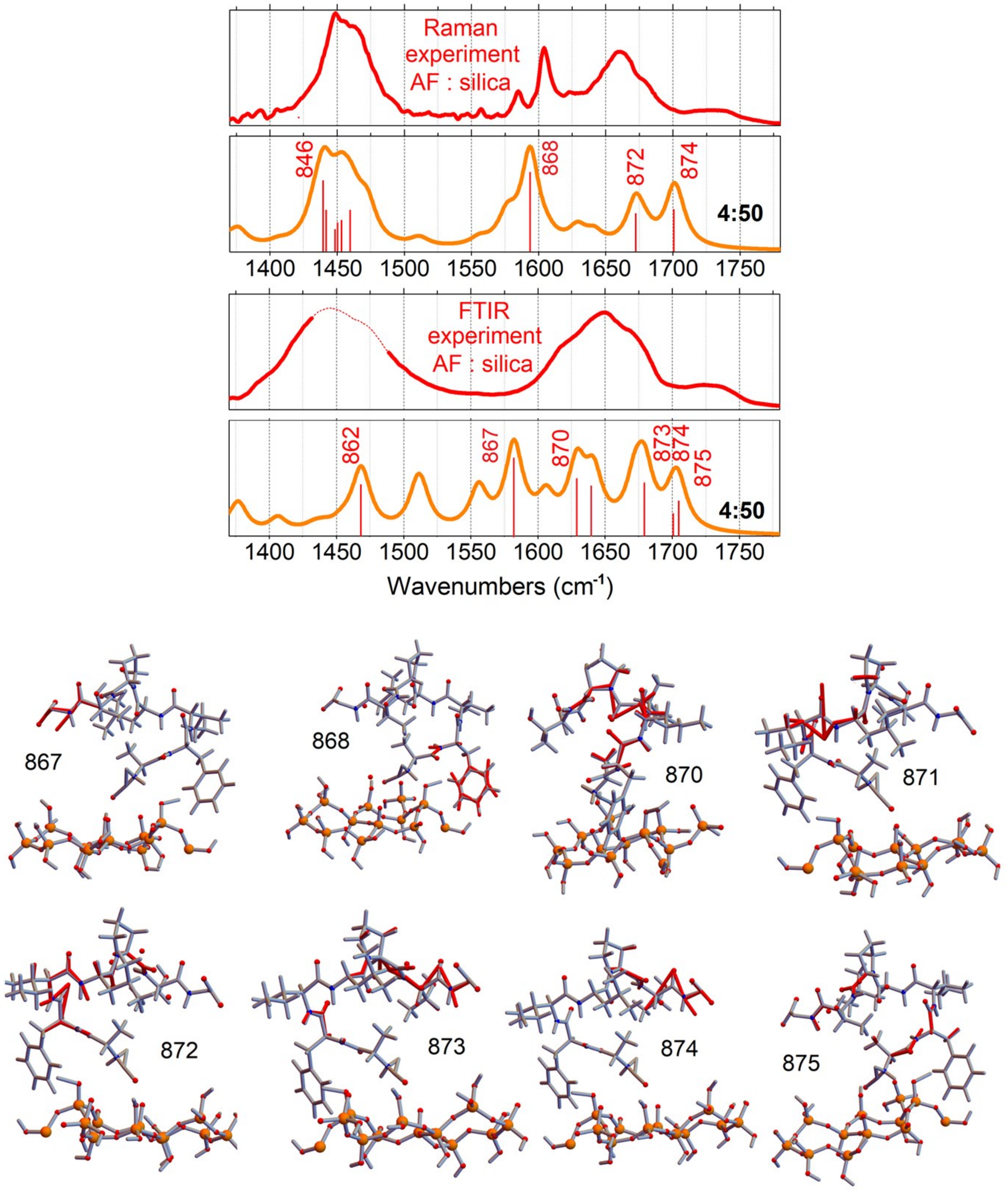

Figure S13. *Experimental Raman and FTIR spectra for the AF polypeptide in presence of silica nanoparticles (red dispersions); DFT predictions of the responses of the computed structural case AF82_4:50 at silica surface (orange line dispersions). Vertical red lines in the panels of the computed dispersions indicate intensities and scaled frequencies of the relevant computed normal modes as described in the visual presentations below according to the normal mode numbering as computed for the structure. Orange spheres indicate position of silica atoms. For clarity of normal mode demonstrations, we removed water molecules.*

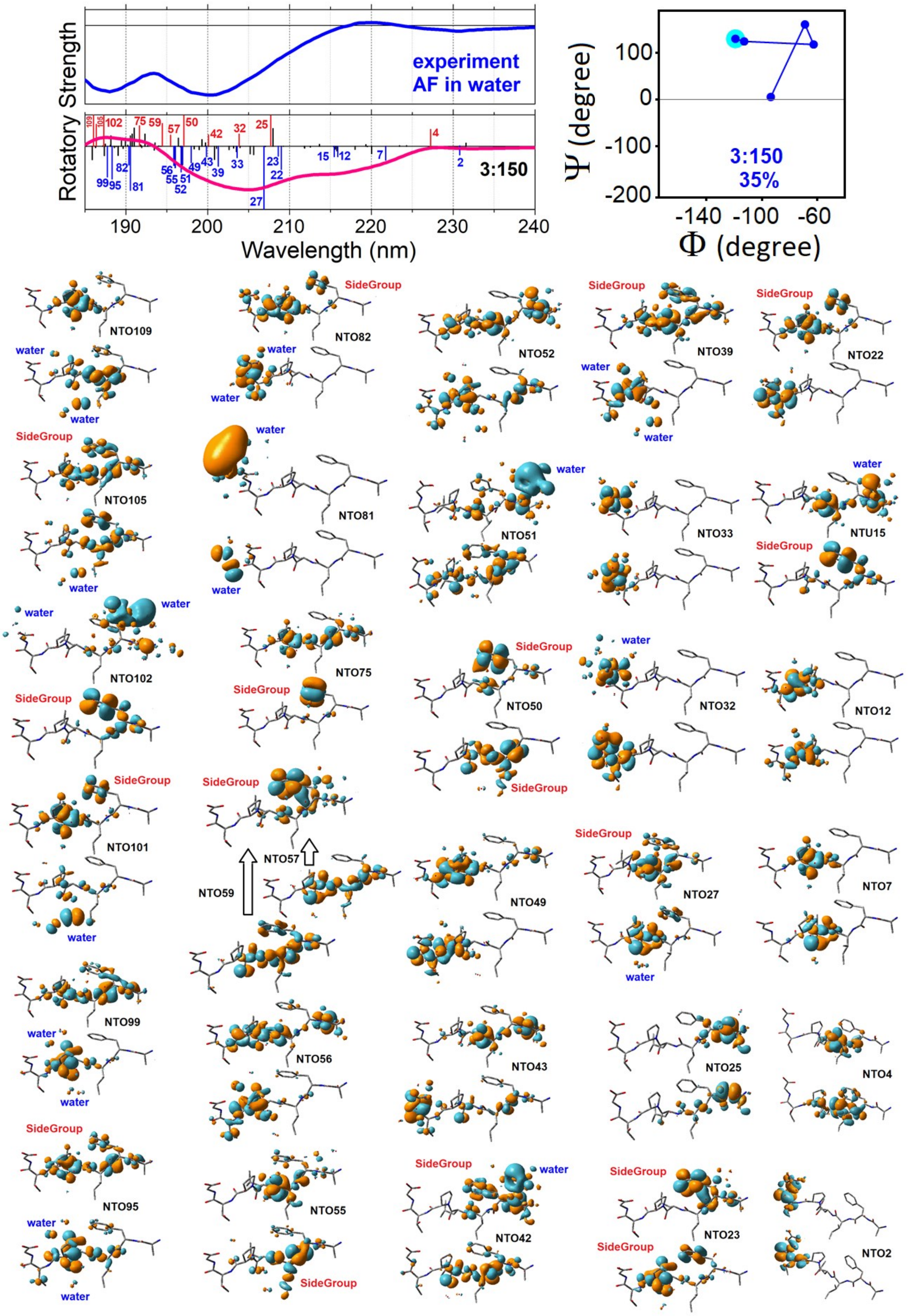

Figure S14. *Experimental CD spectrum in water (blue line dispersion) and DFT prediction for the aqueous AF82_3:150 structural case (purple line dispersions) and Ramachandran space description for the backbone. Red and Blue vertical lines, in the panel of the simulated dispersion, are the positive and negative optical activities computed for the most relevant electronic transitions by the NTO pairs as described in the visual presentations below. For clarity, we removed water molecules which do not contribute.*

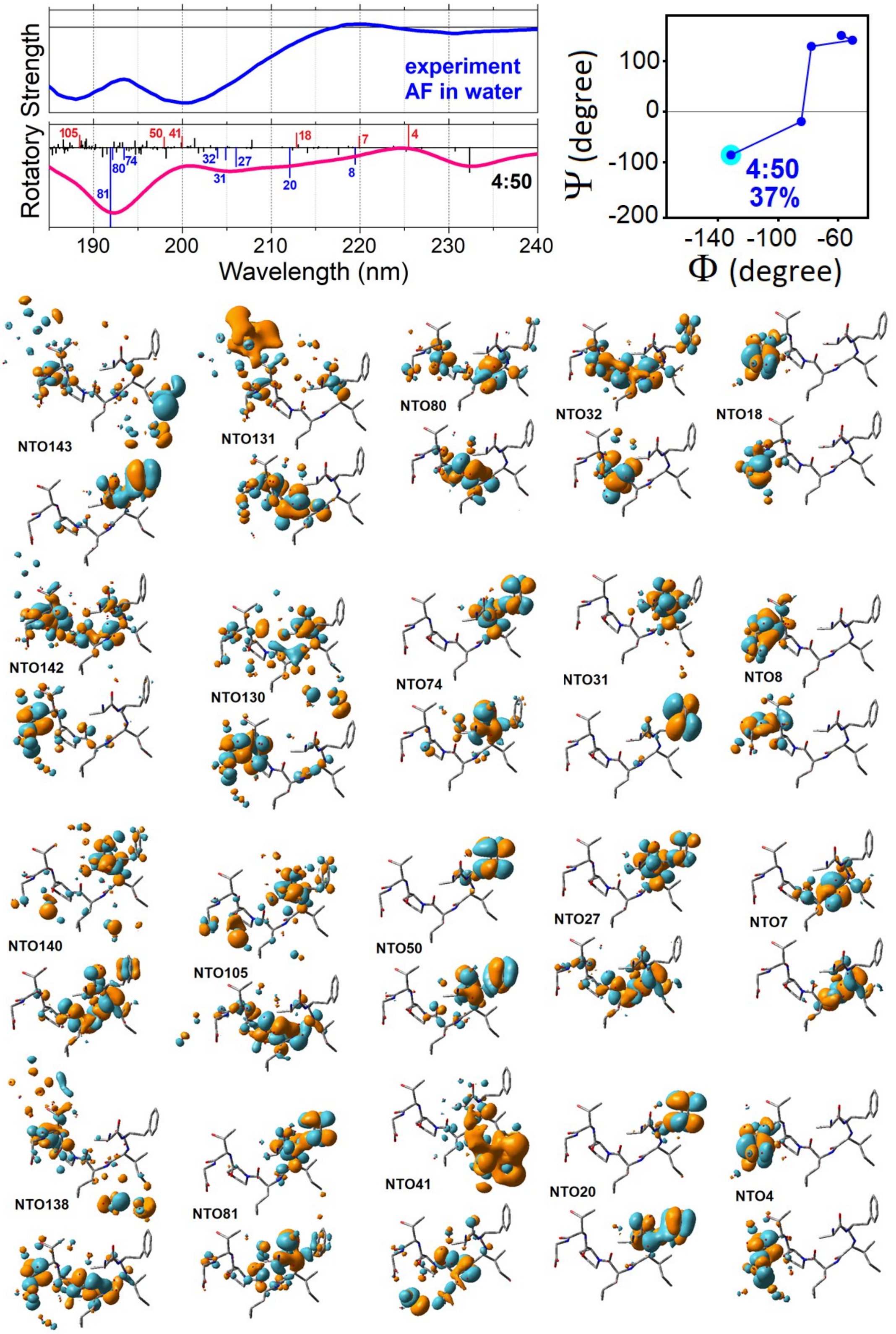

Figure S15. *Experimental CD spectrum in water (blue line dispersion) and DFT prediction for the aqueous AF82_4:50 structural case (purple line dispersion) and Ramachandran space description for the backbone. Red and Blue vertical lines, in the panel of the simulated dispersion, are the positive and negative optical activities computed for the most relevant electronic transitions by the NTO pairs as described in the visual presentations below. For clarity, we removed water molecules which do not contribute.*

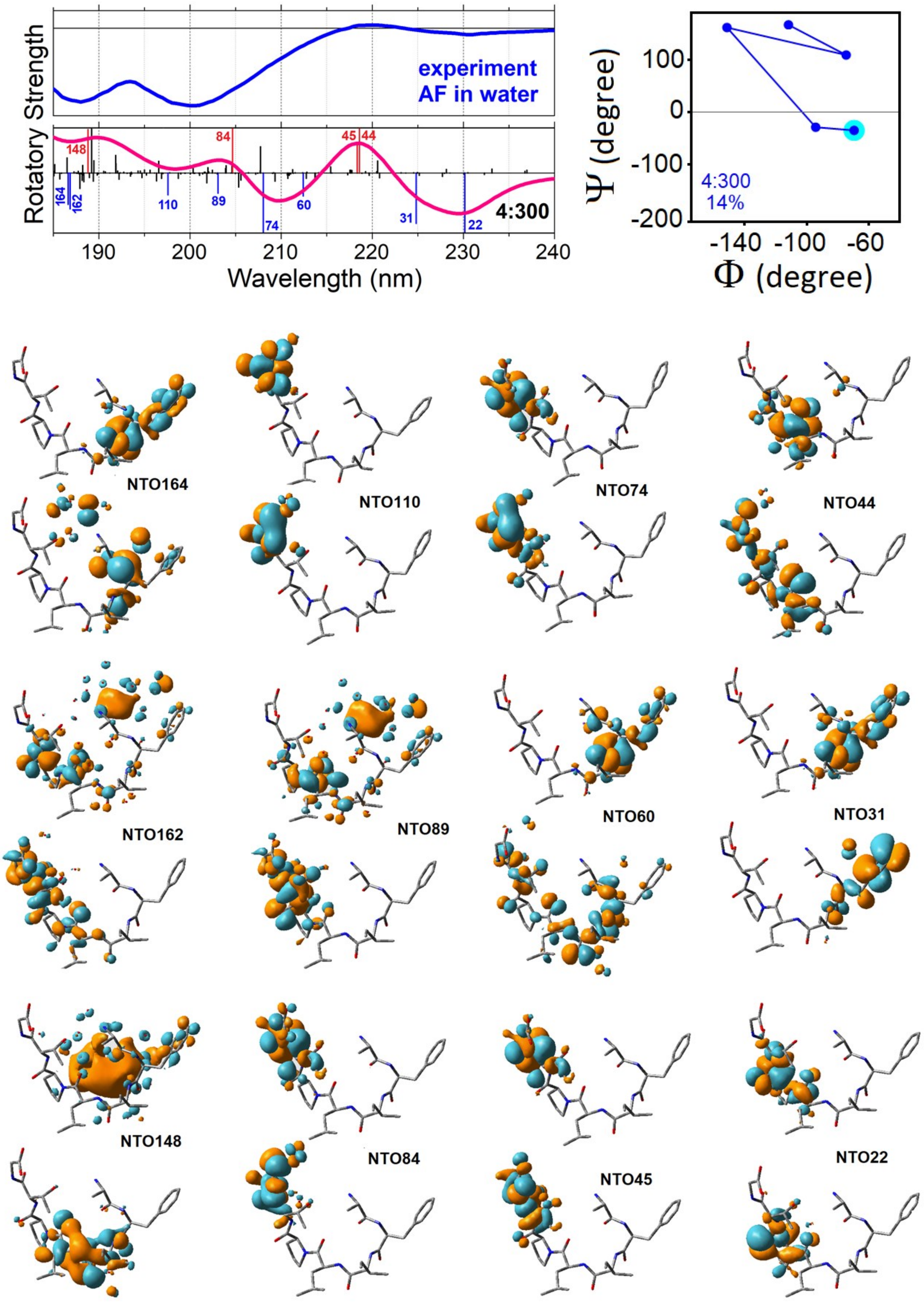

Figure S16. *Experimental CD spectrum in water (blue line dispersion) and DFT prediction for the aqueous AF82_4:300 structural case (purple line dispersion) and Ramachandran space description for the backbone. Red and Blue vertical lines, in the panel of the simulated dispersion, are the positive and negative optical activities computed for the most relevant electronic transitions by the NTO pairs as described in the visual presentations below. For clarity, we removed water molecules which do not contribute.*

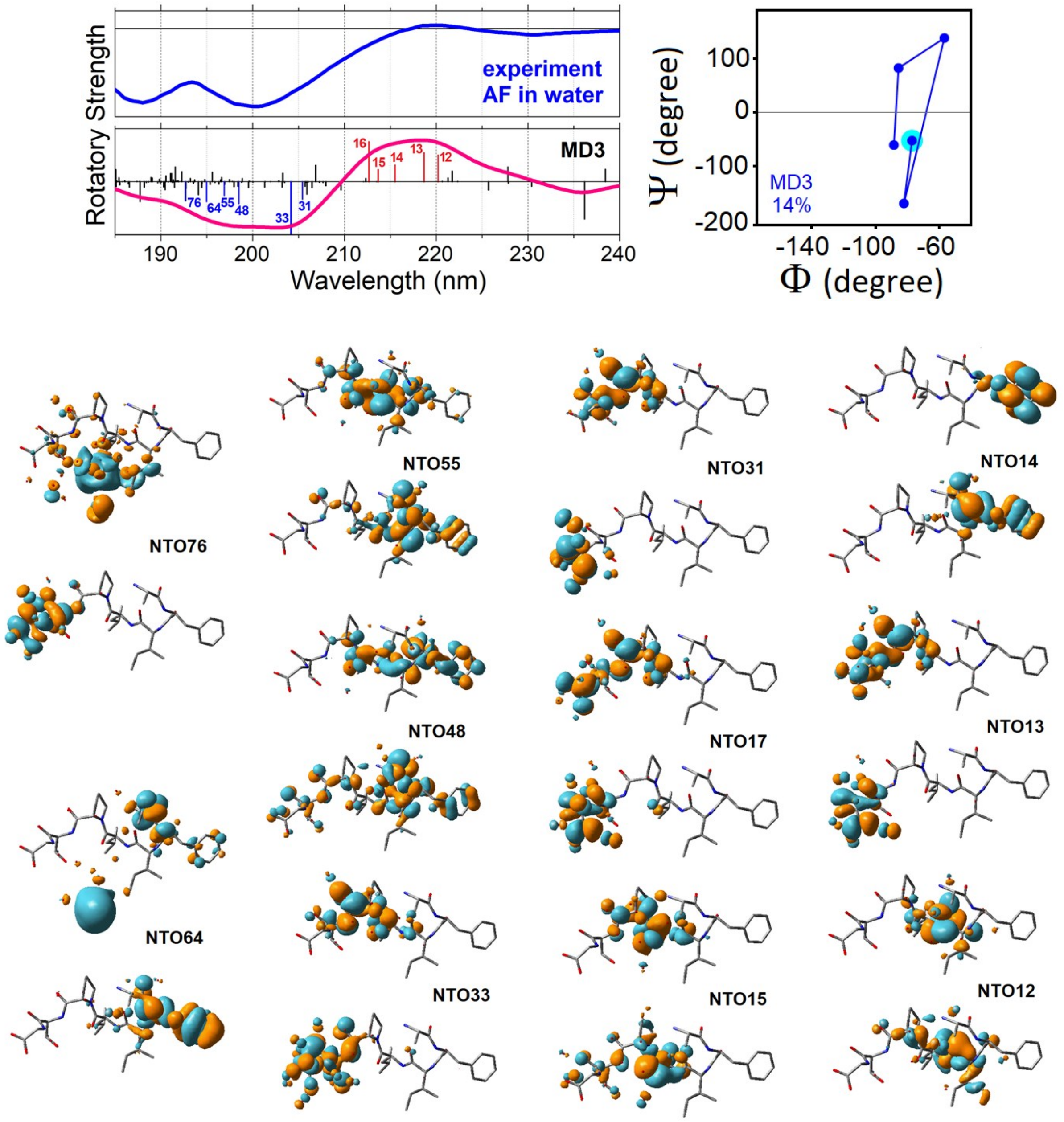

Figure S17. *Experimental CD spectrum in water (blue line dispersion) and DFT prediction for the aqueous MD3 structural case (purple line dispersion) and Ramachandran space description for the backbone. Red and Blue vertical lines, in the panel of the simulated dispersion, are the positive and negative optical activities computed for the most relevant electronic transitions by the NTO pairs as described in the visual presentations below. For clarity, we removed water molecules which do not contribute.*

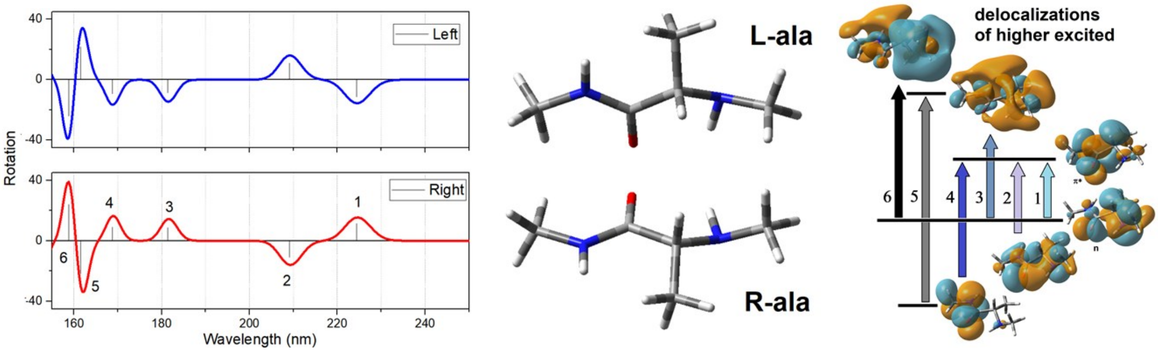

Figure S18. *TD-DFT computed CD spectra of six lowest electronic transitions of a model methylated L and R alanine, as indicated. Six NTO pairs of the model methylated L-alanine.*

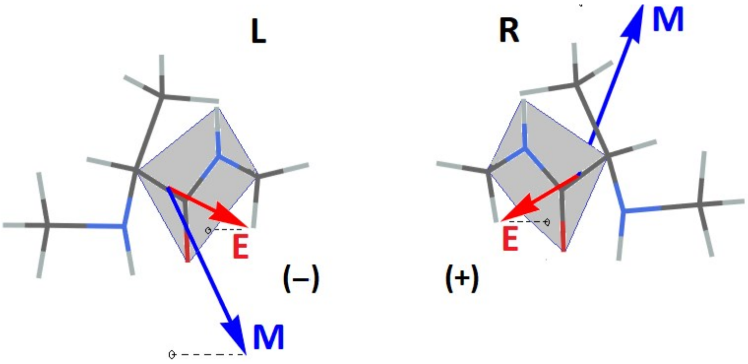

Figure S19. *Orientations of TD-DFT computed transition electric (red) and magnetic (blue) dipole moments for the lowest energy (least delocalized) transition of the model methylated L and R alanine in respect to the plane of the amide units.*

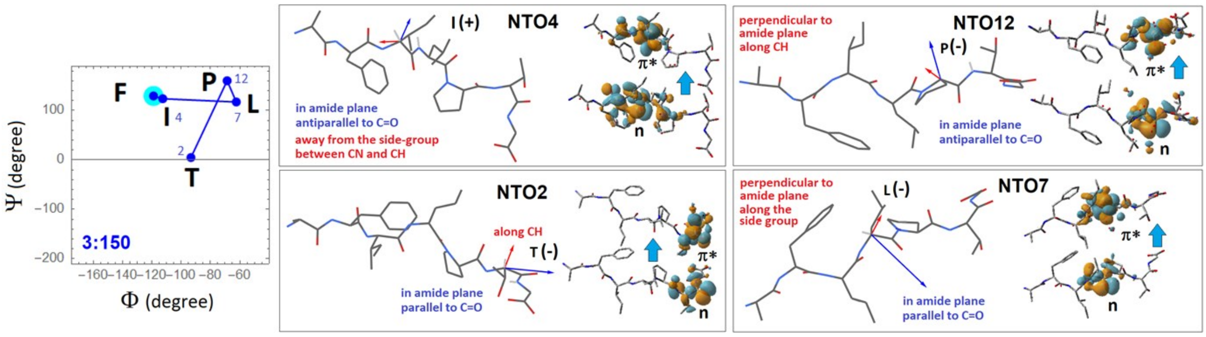

Figure S20. *Orientations of the computed transition electric (red) and magnetic (blue) transition dipole moments for the n→π* excitations described by the NTO pairs 2, 4, 7, 12 and localised on the amide units of the threonine, isoleucine, leucine and proline, respectively, for the simulated structure AF82_3:150.*

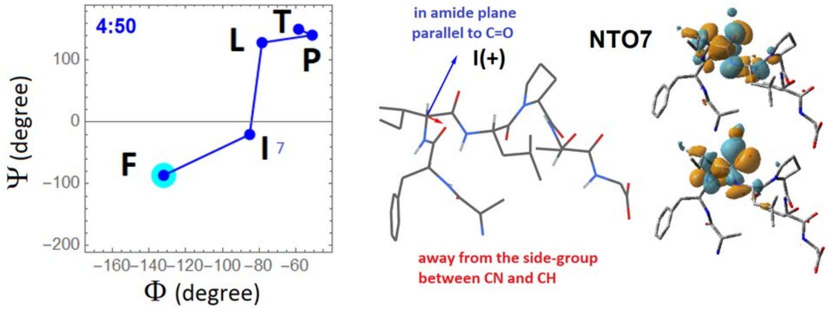

Figure S21. *Orientations of the computed transition electric (red) and magnetic (blue) transition dipole moments for the n→π* excitations, described by the NTO pair 7, localised on the amide units of the isoleucine for the simulated structure AF82_4:50.*

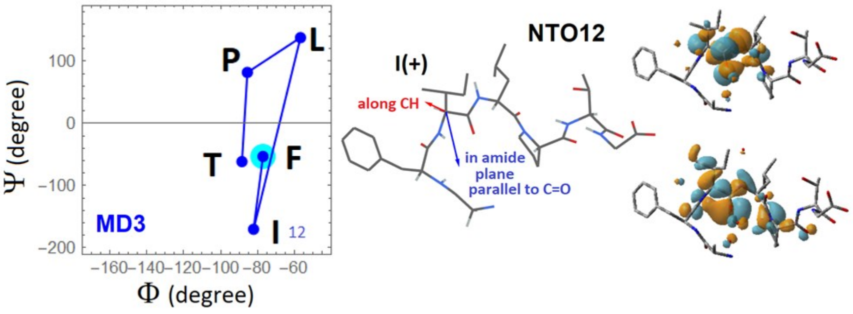

Figure S22. *Orientations of the computed transition electric (red) and magnetic (blue) transition dipole moments for the n→π* excitations, described by the NTO pair 12, localised on the amide units of the isoleucine for the simulated structure MD3.*

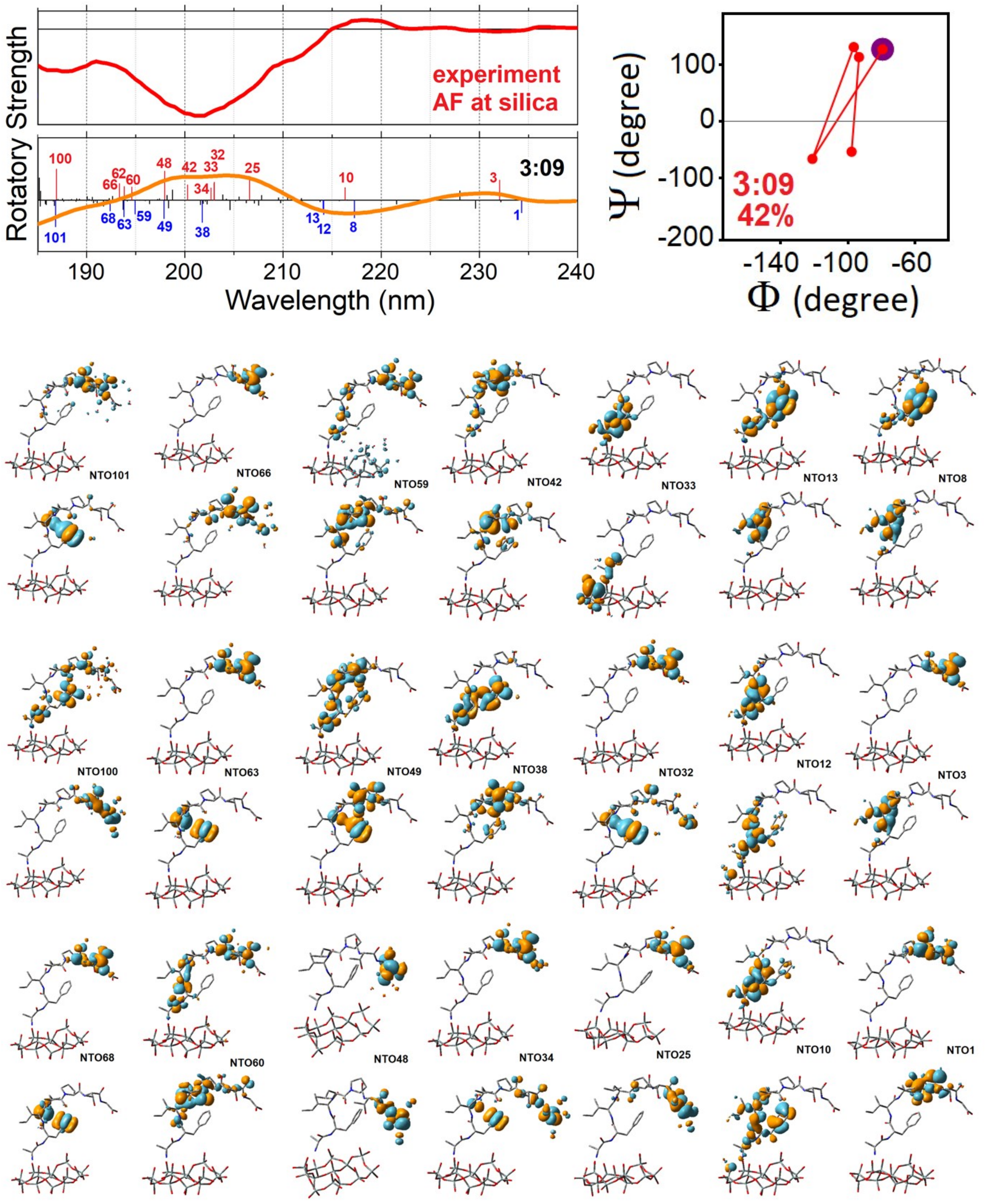

Figure S23. *Experimental CD spectrum in presence of silica nanoparticles (red line dispersion) and DFT prediction for the AF91_3:09 structural case next to silica (orange line dispersion) and Ramachandran space description for the backbone. Red and Blue vertical lines, in the panel of the simulated dispersion, are the positive and negative optical activities computed for the most relevant electronic transitions by the NTO pairs as described in the visual presentations below. For clarity, we removed water molecules which do not contribute.*

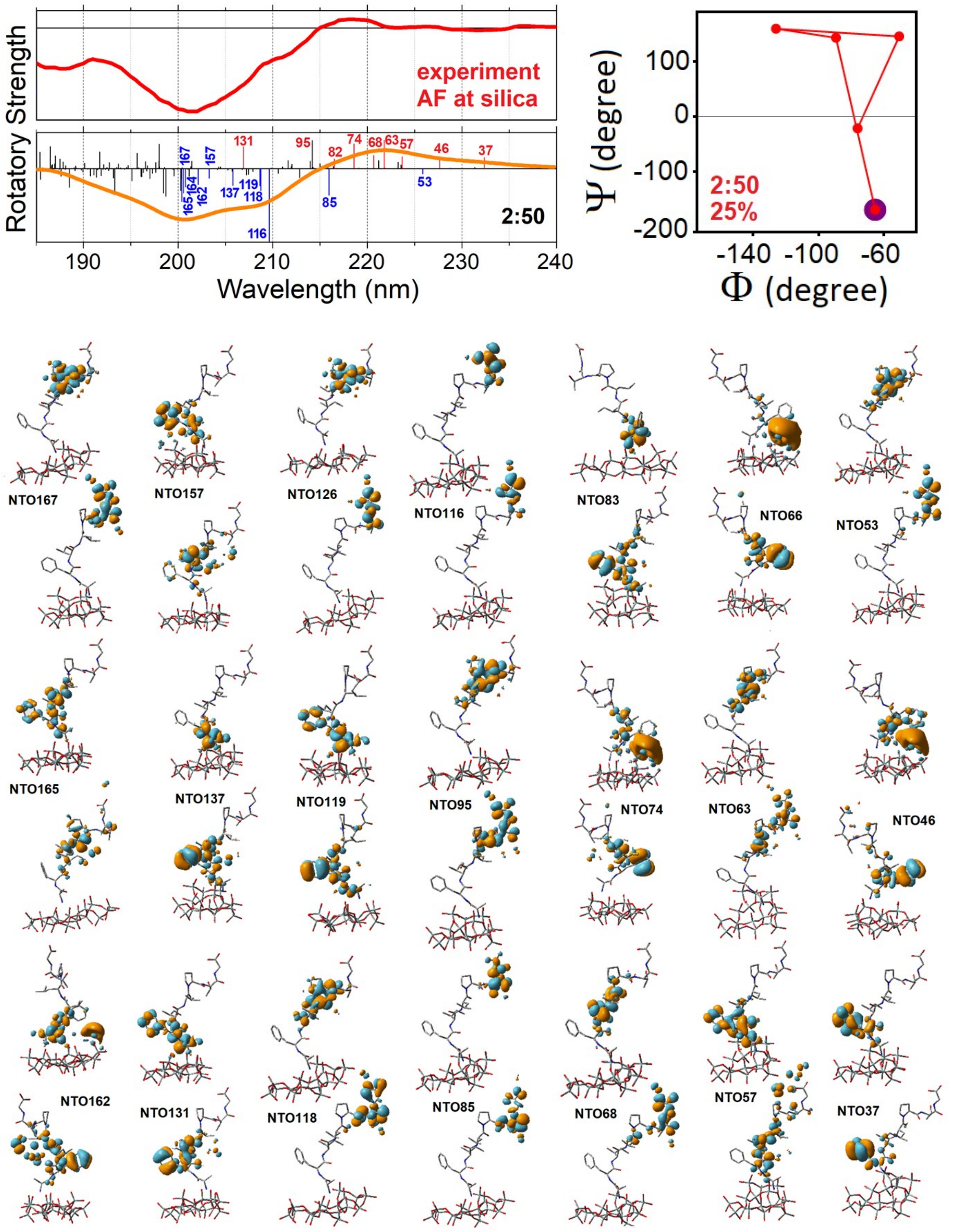

Figure S24. *Experimental CD spectrum in presence of silica nanoparticles (red line dispersion) and DFT prediction for the AF82_2:50 structural case next to silica (orange line dispersion) and Ramachandran space description for the backbone. Red and Blue vertical lines, in the panel of the simulated dispersion, are the positive and negative optical activities computed for the most relevant electronic transitions by the NTO pairs as described in the visual presentations below. For clarity, we removed water molecules which do not contribute.*

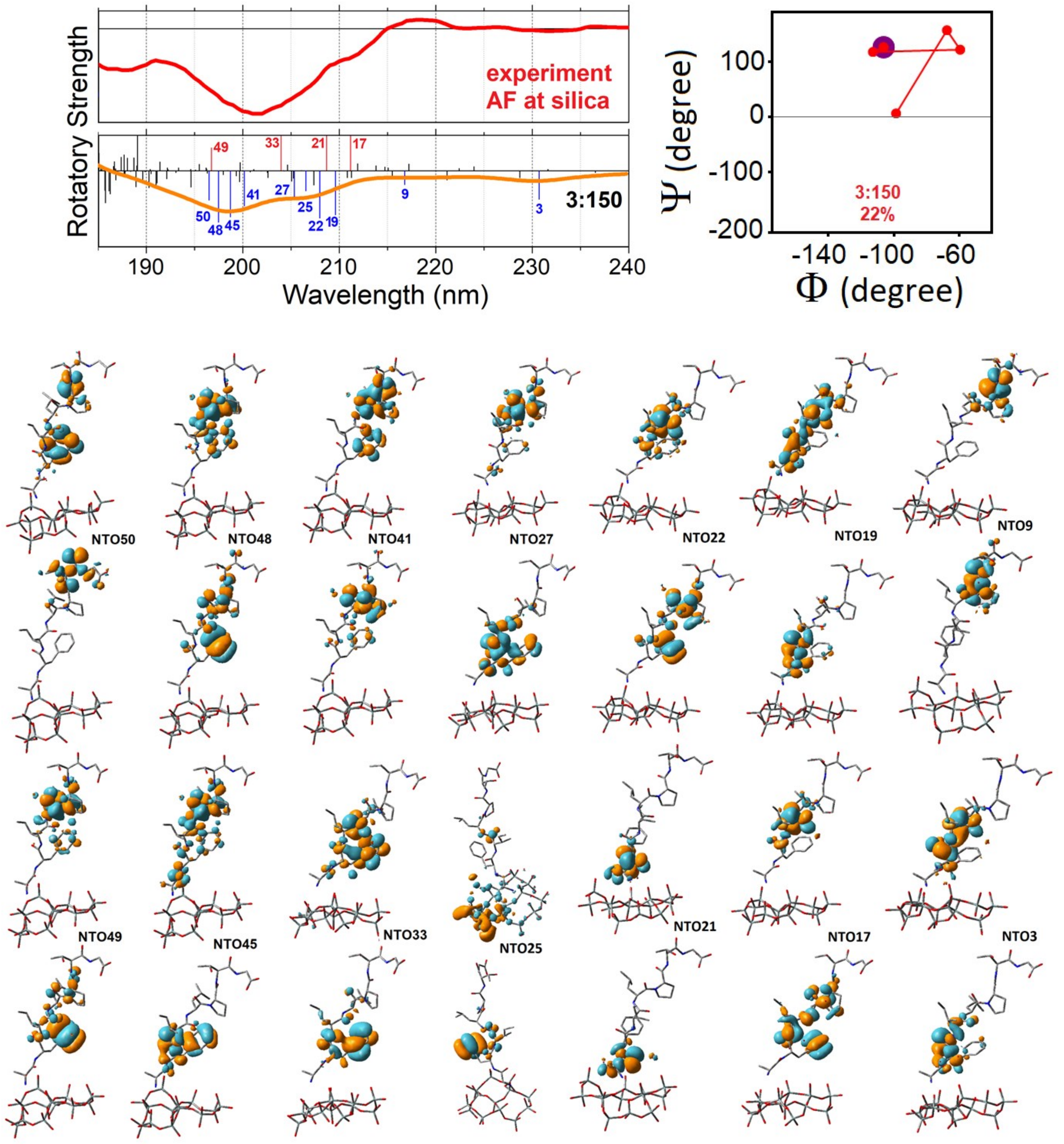

Figure S25. *Experimental CD spectrum in presence of silica nanoparticles (red line dispersion) and DFT prediction for the AF82_3:150 structural case next to silica (orange line dispersion) and Ramachandran space description for the backbone. Red and Blue vertical lines, in the panel of the simulated dispersion, are the positive and negative optical activities computed for the most relevant electronic transitions by the NTO pairs as described in the visual presentations below. For clarity, we removed water molecules which do not contribute.*

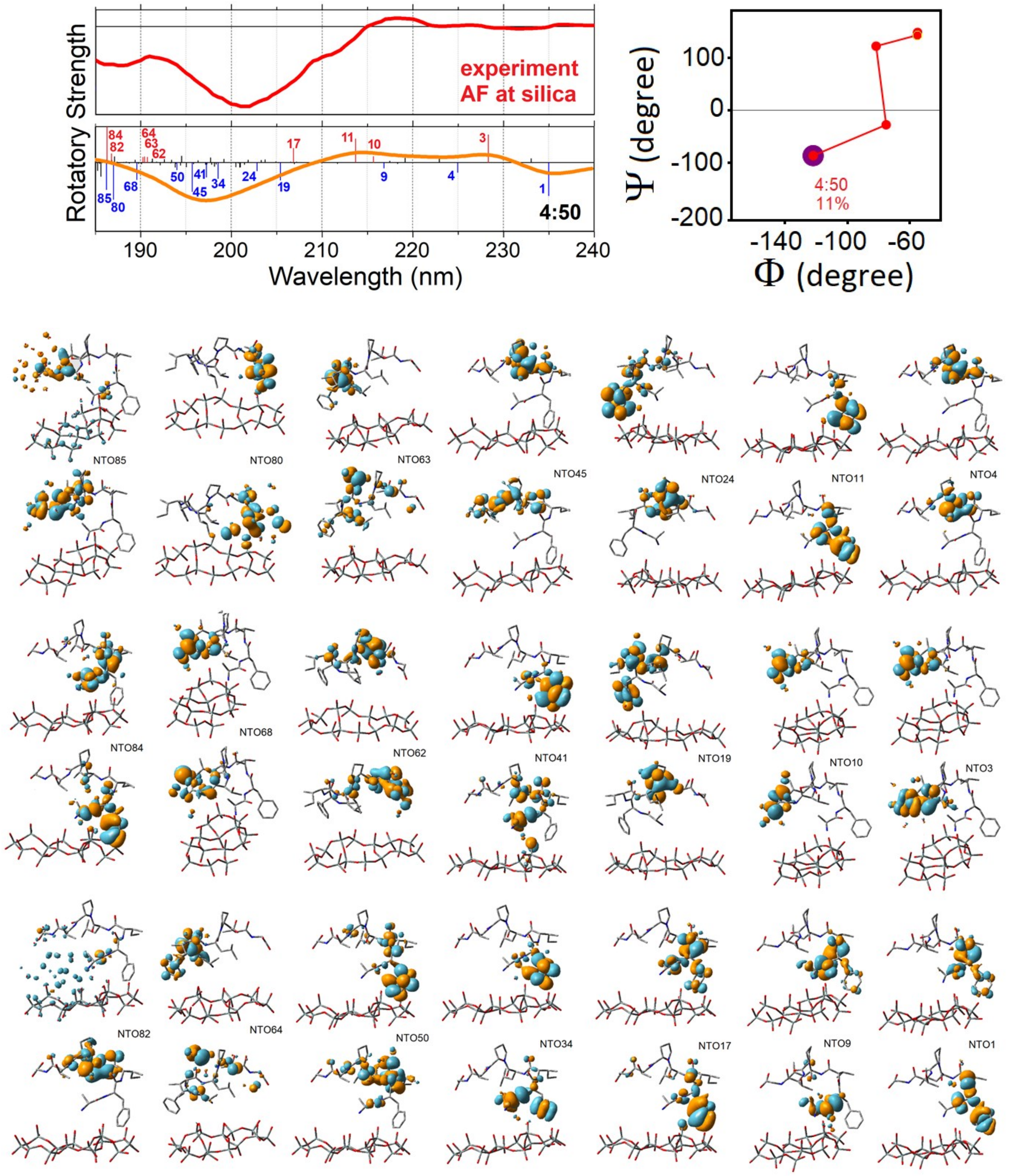

Figure S26. *Experimental CD spectrum in presence of silica nanoparticles (red line dispersion) and DFT prediction for the AF82_4:50 structural case next to silica (orange line dispersion) and Ramachandran space description for the backbone. Red and Blue vertical lines, in the panel of the simulated dispersion, are the positive and negative optical activities computed for the most relevant electronic transitions by the NTO pairs as described in the visual presentations below. For clarity, we removed water molecules which do not contribute.*

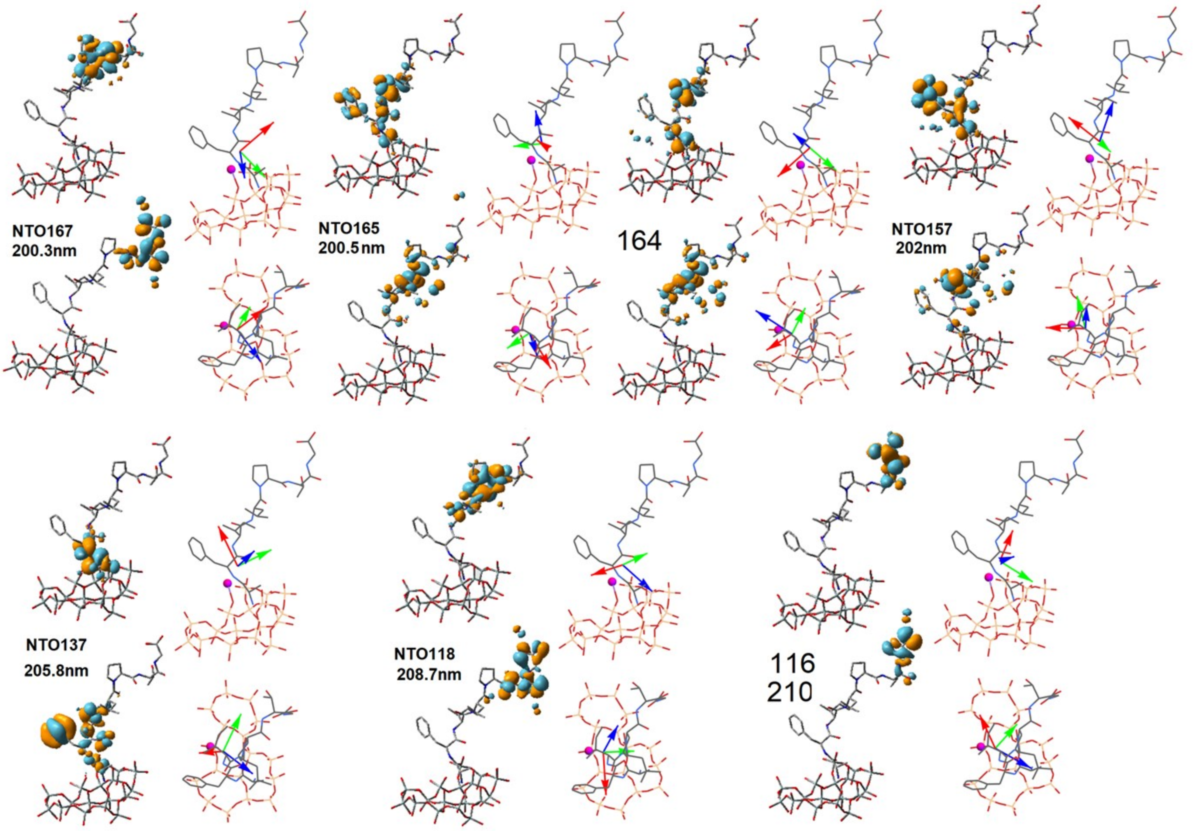

Figure S27. *View from the side and from the top on the orientation of the computed transition electric (red) and magnetic (blue) transition dipole moments for the excitations described by the NTO pair, as indicated, for the structure AF82_2:50 when next to silica. Green vectors are the eye-guides computed as vector products of the corresponding electric and magnetic component.*

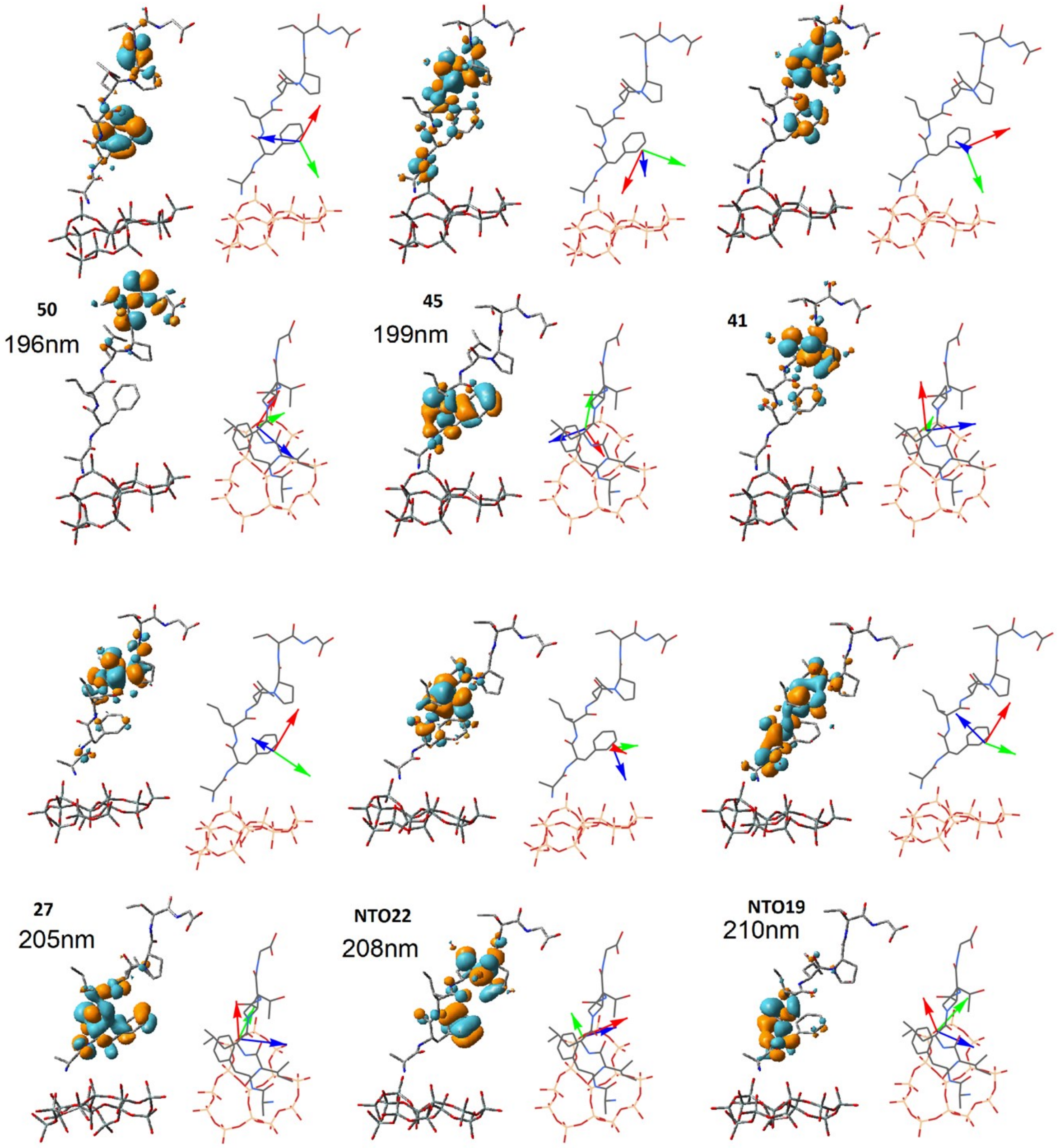

Figure S28. *Orientation of the computed transition electric (red) and magnetic (blue) transition dipole moments for the excitations described by the NTO pair, as indicated, for the structure AF82_3:150 when next to silica. Green vectors are the eye-guides computed as vector products of the corresponding electric and magnetic component.*